

磁控溅射法制备PMN-PZT/PZT异质薄膜的电性能

宛瑛泽, 李克洪, 孟令凤, 张 帅, 杨志峰, 邹赫麟*

大连理工大学, 辽宁 大连

收稿日期: 2022年4月21日; 录用日期: 2022年5月18日; 发布日期: 2022年5月25日

摘 要

在Pt(111)/Ti/SiO₂/Si(100)基底上覆盖Pb_{1.2}(Zr_{0.40}, Ti_{0.60})O₃种子层, 使用磁控溅射法在种子层上交替沉积0.3Pb(Mg_{1/3}Nb_{2/3})O₃-0.7Pb(Zr_{0.52}Ti_{0.48})O₃和Pb(Zr_{0.52}Ti_{0.48})O₃制备多层异质结构薄膜。研究异质界面数量不变的基础上, 0.3Pb(Mg_{1/3}Nb_{2/3})O₃-0.7Pb(Zr_{0.52}Ti_{0.48})O₃和Pb(Zr_{0.52}Ti_{0.48})O₃厚度比变化对PZT性能的影响。通过XRD测得所有薄膜具备单一的钙钛矿相和(111)择优取向。使用扫描电子显微镜(SEM)观察到多层薄膜呈现致密的没有明显缺陷的钙钛矿结构。研究发现, 在PMN-PZT和PZT的厚度比为2:1的条件下介电性能达到最佳, 在频率为1 kHz时测得 $\epsilon_r = 1237.9$, $\tan\delta = 0.048$ 。使用标准铁电测试系统测得PMN-PZT和PZT的厚度比为的样品呈现饱和的P-E滞后曲线。此外, 测得在电场下, PMN-PZT和PZT的厚度比为2:1的多层异质薄膜具有最小的漏电流密度为 $J = 5.5 \times 10^{-8} \text{ A/cm}^2$ 。

关键词

磁控溅射, 多层PZT薄膜, 厚度比, 微观结构, 电性能

Electrical Properties of PMN-PZT/PZT Heterostructure Films Prepared by Magnetron Sputtering

Yingze Wan, Kehong Li, Lingfeng Meng, Shuai Zhang, Zhifeng Yang, Helin Zou*

Dalian University of technology, Dalian Liaoning

Received: Apr. 21st, 2022; accepted: May 18th, 2022; published: May 25th, 2022

Abstract

Pb_{1.2}(Zr_{0.40}, Ti_{0.60})O₃ was covered on Pt(111)/Ti/SiO₂/Si(100) substrate seed layer. Multilayer heterostructure films were prepared by magnetron sputtering. The influence of the thickness ratio of 0.3Pb(Mg_{1/3}Nb_{2/3})O₃-0.7Pb(Zr_{0.52}Ti_{0.48})O₃ and Pb(Zr_{0.52}Ti_{0.48})O₃ on the electrical properties of PZT was studied on the basis of the constant number of heterostructure interfaces. XRD measured that all the films had a single perovskite phase and (111) preferred orientation. SEM observed that the multilayer films presented dense perovskite structure without obvious defects. It was found that the dielectric properties of PMN-PZT and PZT reached the best when the thickness ratio of PMN-PZT and PZT was 2:1. At a frequency of 1 kHz, the measured $\epsilon_r = 1237.9$ and $\tan\delta = 0.048$. Using a standard ferroelectric test system, the samples with the thickness ratio of PMN-PZT and PZT presented saturated P-E hysteresis curves. In addition, the measured leakage current density of the multilayer heterostructure films with a thickness ratio of 2:1 was $J = 5.5 \times 10^{-8} \text{ A/cm}^2$.

*通讯作者。

文章引用: 宛瑛泽, 李克洪, 孟令凤, 张帅, 杨志峰, 邹赫麟. 磁控溅射法制备 PMN-PZT/PZT 异质薄膜的电性能[J]. 材料科学, 2022, 12(5): 516-523. DOI: 10.12677/ms.2022.125054

rostructure films were prepared by alternately depositing $0.3\text{Pb}(\text{Mg}_{1/3}\text{Nb}_{2/3})\text{O}_3$ - $0.7\text{Pb}(\text{Zr}_{0.52}\text{Ti}_{0.48})\text{O}_3$ and $\text{Pb}(\text{Zr}_{0.52}\text{Ti}_{0.48})\text{O}_3$ on the seed layer by magnetron sputtering. The effects of the thickness ratio of $0.3\text{Pb}(\text{Mg}_{1/3}\text{Nb}_{2/3})\text{O}_3$ - $0.7\text{Pb}(\text{Zr}_{0.52}\text{Ti}_{0.48})\text{O}_3$ and $\text{Pb}(\text{Zr}_{0.52}\text{Ti}_{0.48})\text{O}_3$ on the properties of PZT were studied. All films have a single perovskite phase and (111) preferred orientation measured by XRD. Scanning electron microscopy (SEM) showed that the multilayer films showed a dense perovskite structure without obvious defects. It is found that the dielectric properties reach the best when the thickness ratio of PMN-PZT to PZT is 2:1, which is measured at the frequency of 1 kHz $\epsilon_r = 1237.9$, $\tan\delta = 0.048$. The sample measured by standard ferroelectric test system shows a saturated P-E hysteresis curve of 2:1. In addition, it is measured that the multilayer heterostructure film with thickness ratio of 2:1 has the minimum leakage current density of $J = 5.5 \times 10^{-8} \text{ A/cm}^2$.

Keywords

Magnetron Sputtering, Multilayer PZT Film, Thickness Ratio, Microstructure, Electrical Properties

Copyright © 2022 by author(s) and Hans Publishers Inc.

This work is licensed under the Creative Commons Attribution International License (CC BY 4.0).

<http://creativecommons.org/licenses/by/4.0/>



Open Access

1. 介绍

锆钛酸铅(PZT)薄膜因铁电、介电以及压电特性优异,广泛应用于铁电存储器、可穿戴设备等多领域的研究当中[1][2]。目前 PZT 薄膜的制备常用金属有机化学气相沉积(MOCVD)法、溅射法、脉冲激光法(MOCVD)、溶胶凝胶法(Sol-Gel)等[3]-[14]。其中,由于成型速度高、结晶良好,RF 磁控溅射被广泛应用。

众多学者对于可能影响薄膜性能的因素[15][16][17]进行研究发现,掺杂[7]、制备缓冲层以及制备多层薄膜等方法均能改善 PZT 薄膜的性能。组分不同的薄膜通过交替沉积的方法生成多层异质薄膜结构也越来越受到关注[18]-[23]。Wang F 等人发现掺杂浓度为 0.1% 的 Ce 离子的 PZT 薄膜具有优异的电性能。在 0.1 kHz 时, ϵ_r 和 $\tan\delta$ 分别为 1326.9 和 0.063, $2Pr$ 为 $13.58 \mu\text{C/cm}^2$, 比未掺杂 Ce 离子的样品提高 42.4%。Wu J 等人利用磁控溅射法在 Pt 上先后沉积了 PbO 缓冲层和 PZT 薄膜,制备出较高(100)择优取向的薄膜,电性能明显提高。Huiting S 等人制备了 PMN-PT/PZT 多层异质结构薄膜, ϵ_r 和 $\tan\delta$ 分别为 1959 和 0.0152。在 400 kV/cm 电场强度下,漏电流密度为 $9 \times 10^{-8} \text{ A/cm}^2$ 。表现出优异的介电和铁电性能。

本次工作中,先在 Pt/Ti/SiO₂/Si 衬底上利用溶胶凝胶法制备了 $\text{Pb}_{1.2}(\text{Zr}_{0.40}, \text{Ti}_{0.60})\text{O}_3$ 种子层,然后在其采用原位溅射法沉积 $0.3\text{Pb}(\text{Mg}_{1/3}\text{Nb}_{2/3})\text{O}_3$ - $0.7\text{Pb}(\text{Zr}_{0.52}\text{Ti}_{0.48})\text{O}_3$ /Pb($\text{Zr}_{0.52}\text{Ti}_{0.48}$) O_3 (PMN-PZT/PZT)异质薄膜,具体参数如表 1 所列。沉积步骤如下:将 PZT、PMN-PZT 靶材装在腔室内相应位置,依次交替沉积,控制每层厚度比分别为 1:2、1:3、3:1、2:1,形成异质界面数量为 5,厚度约 700 nm 的多层异质结构薄膜,制备 PZT 和 PMN-PZT 薄膜作为对照组,异质结构薄膜示意图如图 1 所示。

2. 实验步骤

首先,制备 PZT 前驱体溶液,然后用滴管吸取前驱体溶液滴到吸附在托盘上的底电极上,利用旋涂法,低速 600 r/min, 12 s; 高速 2800 r/min, 30 s, 制得 PZT 湿膜,然后将其放置在 150°C 的干燥箱中保温 5 min。然后放入常规马弗炉中 5 min (去水分); 450°C, 5 min (热分解有机物); 600°C, 10 min (退火结晶)。重复上述步骤重得到缓冲层。

Table 1. Magnetron sputtering parameters
表 1. 磁控溅射参数

靶材	PMN-PZT 和 PZT 靶材
靶材直径	60 mm
溅射功率	100 W
靶材 - 衬底间距	100 mm
背底真空度	3.0×10^{-5} Pa
溅射气压	2 Pa
衬底温度	650°C
溅射气氛	O ₂ /Ar 混合气体(10/90)

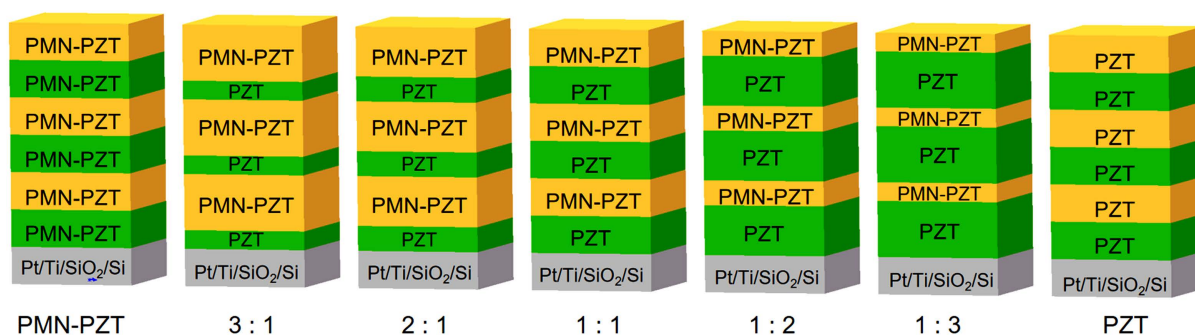


Figure 1. Schematic diagram of PMN-PZT/PZT heterostructure film
图 1. PMN-PZT/PZT 异质结构薄膜示意图

然后，使用磁控溅射法采用原位溅射工艺沉积 $0.3\text{Pb}(\text{Mg}_{1/3}\text{Nb}_{2/3})\text{O}_3-0.7\text{Pb}(\text{Zr}_{0.52}\text{Ti}_{0.48})\text{O}_3/\text{Pb}(\text{Zr}_{0.52}\text{Ti}_{0.48})\text{O}_3$ (PMN-PZT/PZT)异质结构薄膜。对基片进行烘干和去水分。选定 PZT 和 PMN-PZT 两种靶材放置在强室内相应位置，将制备好的基底装入样品台，待腔室内真空度达到 5.0×10^{-5} Pa 后，通入氧氩混合气体，利用节流阀稳定气压；射频电源功率设置为 150 W，开启射频匹配器，开始交替溅射多层异质薄膜，溅射时 Ar 的气体流量为 90 sccm，腔室气压为 2 Pa，样品台和靶材间的距离保持 100 mm。先沉积 PZT，再沉积 PMN-PZT，交替沉积异质薄膜。表 1 列举了 PZT 薄膜的制备参数。

本文选用 X 射线衍射仪(D8 Bruker, Cu-K α radiation, Bruker, Germany)布拉格角范围 $20^\circ \leq 2\theta \leq 60^\circ$ 内，分析多层异质薄膜的晶体结构和结晶取向。薄膜微观形貌的表征选用扫描电子显微镜(SU8220, Hitachi, Japan)进行表征。使用阻抗分析仪(4294A, Agilent Technologies, US)测量 PZT 薄膜的介电性能，频率函数在 0.1 到 100 KHz 变化。多层异质薄膜的铁电性能使用标准铁电测试系统(Radiant Technologies)测量。

3. 结果和讨论

图 2 为 PMN-PZT/PZT 异质薄膜以及单一组分的 PZT 和 PMN-PZT 薄膜的 XRD 图谱。由图可知，纯 PMN-PZT 薄膜、PMN-PZT 和 PZT 的厚度比分别为 1:2、1:3、3:1 和 2:1 型 PMN-PZT/PZT 异质薄膜均表现为高(111)择优取向的纯钙钛矿相。薄膜的择优取向程度可用以下公式定量表达[24]:

$$\alpha(111) = \frac{I(111)}{I(100) + I(110) + I(111)} \quad (1)$$

公式中的 $I(100)$ 和 $I(111)$ 分别表示(100)和(111)峰的衍射强度。当 PMN-PZT 与 PZT 的厚度比小于 2:1 时, 异质薄膜的(111)择优取向度较高是由于 Mg、Nb 含量能够影响薄膜的晶向结构。如最低表面能理论所述 [25], 掺 Mg、Nb 能够促进 PZT 薄膜优先沿着(111)晶面成长, 同时抑制其他取向的形核与生长。但随着 PMN-PZT 与 PZT 的厚度比到达 3:1, 过量的 Mg、Nb 无法全部进入 PZT 薄膜的晶格之中, 在边界处产生聚集, PZT 薄膜沿着(111)取向的形核生长受到抑制, 导致异质薄膜的(111)择优取向度减小。此外, 异质成核也会促进 PZT 薄膜沿择优取向生长。

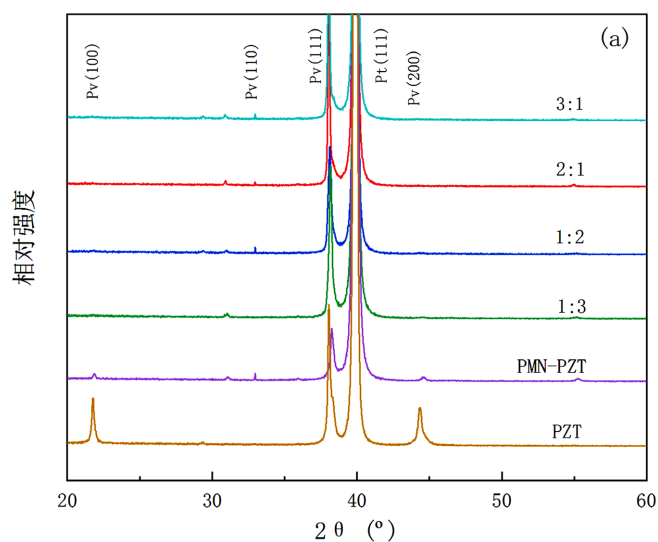
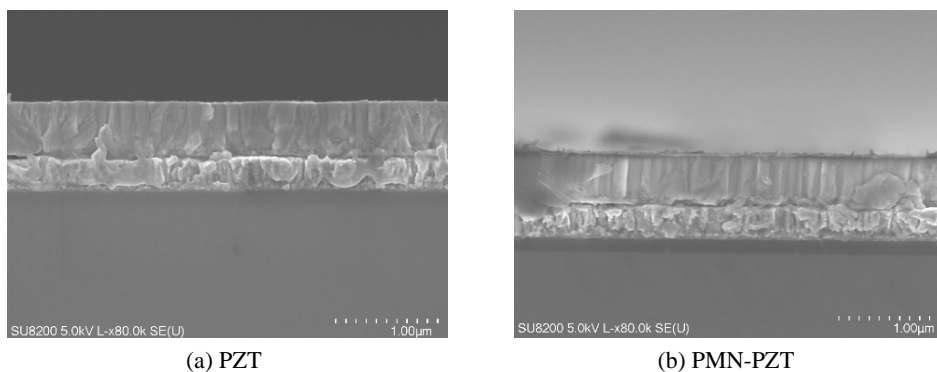


Figure 2. XRD pattern of PMN-PZT/PZT heterogeneous films

图 2. PMN-PZT/PZT 异质薄膜的 XRD 图谱

图 3 为使用 FE-SEM 测得样品的截面形貌。单一组分的 PZT、PMN-PZT 以及 PMN-PZT 和 PZT 厚度比为 2:1 和 3:1 时的异质薄膜截面微观结构如图 3 所示, 缓冲层和其上生长的薄膜之间有着微弱的界面, 薄膜均为钙钛矿结构且柱状结构致密。厚度效应可能会降低钙钛矿结构的结晶驱动力 [26], 进而导致纯 PZT 薄膜的柱状结构随着薄膜厚度的增加而逐渐模糊(图 3(a)所示)。PMN-PZT 相较于纯 PZT 柱状结构相对模糊, 致密性较差, 晶粒较小且表面较为粗糙, 因为离子的替代会对晶粒形核生长产生抑制。由图可看出, PMN-PZT 和 PZT 厚度比为 2:1 时, 异质薄膜晶粒生长良好, 晶界清晰, 薄膜柱状结构致密性最好。研究表明, PMN-PZT 和 PZT 厚度比变化对 PZT 薄膜的界面形貌有显著影响, PMN-PZT 和 PZT 的厚度比(小于等于 2:1)是多层异质结构薄膜表面均匀, 柱状结构更为致密, 而厚度比较大时, 由于 Mg、Nb 离子在晶界处发生聚集, 影响晶粒长大, 导致 PZT 薄膜柱状结构致密程度下降。



(a) PZT

(b) PMN-PZT

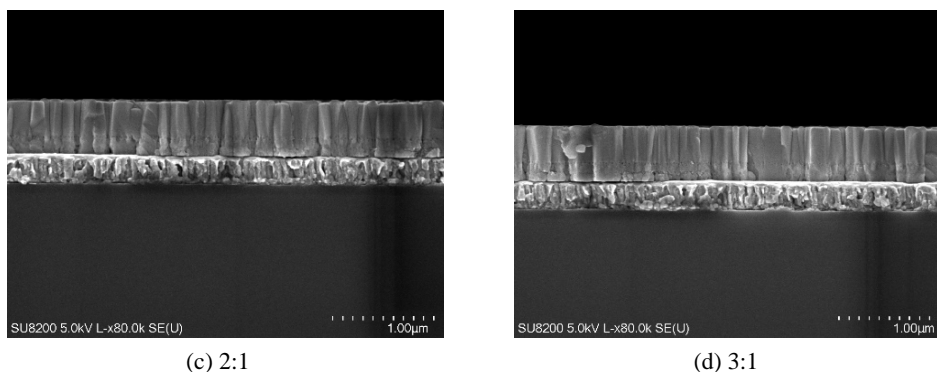


Figure 3. Interface diagram of all samples: (a) PZT; (b) PMN-PZT; (c) 2:1; (d) 3:1

图 3. 所有样品的界面图: (a) PZT; (b) PMN-PZT; (c) 2:1; (d) 3:1

图 4(a)为单一组分的 PZT、PMN-PZT 薄膜以及 PMN-PZT/PZT 异质薄膜的 P-E 回线。图中可以看出，磁滞回线均饱和，如图 4(b)所示，PMN-PZT 和 PZT 的厚度比为 2:1 的样品剩余极化 $Pr = 21 \mu\text{C}/\text{cm}^2$ 和矫顽场强 $Ec = 90 \text{ kV}/\text{cm}$ ，二者均较大。这可能是由于多层异质结构和内应力的改变。此外 PMN-PZT 和 PZT 的厚度比为 2:1 的样品(111)择优取向度较大，因而相对于其他样品而言， Pr 有所提高。PMN-PZT 和 PZT 的厚度比为 2:1 的样品具有最佳的铁电性能。PZT 薄膜的铁电性能在受结晶取向影响的同时，还与薄膜组分有关，因此由于厚度变化造成的离子浓度的改变使得其他样品的铁电性能明显不如 PMN-PZT 和 PZT 的厚度比为 2:1 的样品。层间耦合效应增强能够促进畴壁运动，这也是铁电性能得到提升的原因之一。

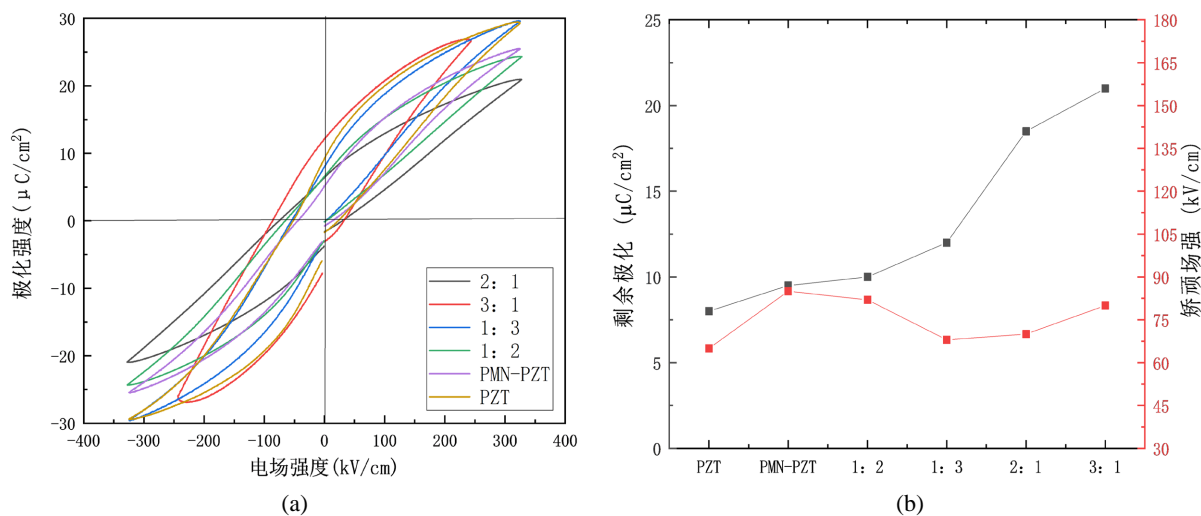


Figure 4. Ferroelectric characteristics of thin film: (a) P-E loop; (b) 2Pr and 2Ec values

图 4. 薄膜铁电特性: (a) P-E 回线; (b) 2Pr 和 2Ec 值

图 5 为制备的异质结构薄膜在 0.1~100 kHz 频率范围内的介电常数和损耗因子变化趋势。从图中可以看出，随着频率的增大多层异质结构薄膜的 ϵ_r 减小， $\tan\delta$ 先减小后增大。PMN-PZT 和 PZT 的厚度比为 2:1 的样品的介电常数最大，在 1 kHz 时， $\epsilon_r = 1237.9$ ，相比于其他厚度比的异质结构薄膜介电常数 ϵ_r 较大介电损耗 $\tan\delta$ 较小。有研究发现极化方向与薄膜的择优生长取向有着一定的关联所以厚度比为 2:1 的样品介电性能的提高可能是由于其高(111)择优取向。由于厚度效应和界面耦合效应的作用，交替沉积的薄膜的电性能会有相应的提高，这也是 PMN-PZT 和 PZT 的厚度比为 2:1 的样品电性能提高的原因。偶极子损耗、自由电荷等也可能是产生这一影响的原因[27]。

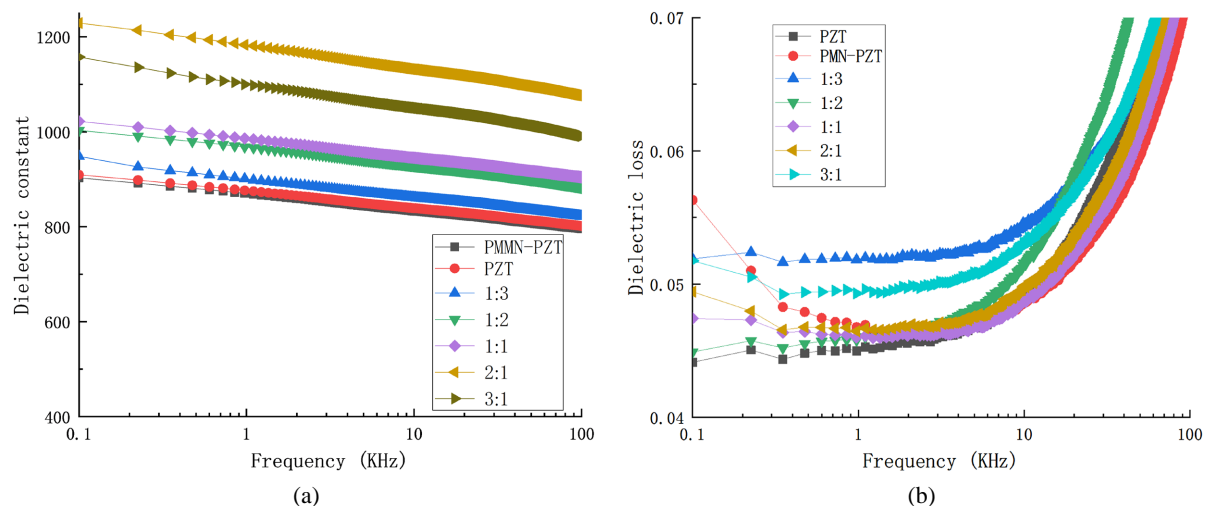


Figure 5. Dielectric properties of thin film: (a) Relationship between dielectric constant and frequency; (b) Relationship between dielectric loss and frequency

图 5. 薄膜介电特性: (a) 介电常数随频率变化关系; (b) 介电损耗随频率变化关系

异质结构薄膜的漏电流密度如图 6 所示。从图中可以看到，漏电流密度随着电场强度的增大而增大。多层薄膜的漏电流密度有所降低。其中，PMN-PZT 样品具有最大的漏电流密度 $9.37 \times 10^{-7} \text{ A/cm}^2$ 。对于多层薄膜样品，随着薄膜交替溅射薄膜厚度的增加，漏电流密度逐渐减小。PMN-PZT 和 PZT 的厚度比为 2:1 相较于 PMN-PZT 和 PZT 的厚度比为 1:3 ($2.67 \times 10^{-7} \text{ A/cm}^2$) 和 PMN-PZT 和 PZT 的厚度比为 1:2 ($8.26 \times 10^{-7} \text{ A/cm}^2$) 的漏电流密度低了接近一个数量级，仅为 $5.5 \times 10^{-8} \text{ A/cm}^2$ 。观察到的 J-E 特性与介电性能测试结果比较符合。

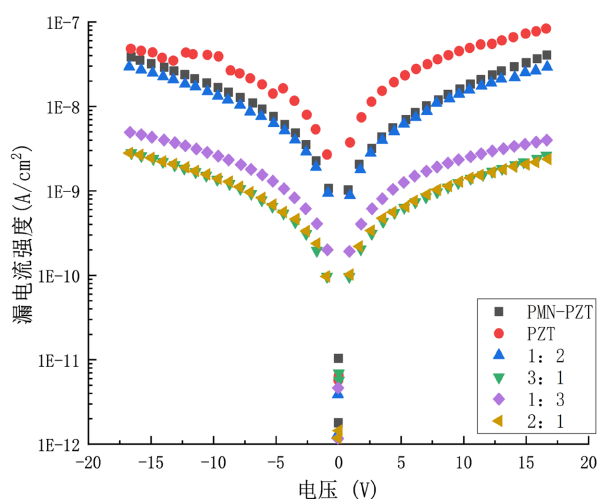


Figure 6. Leakage current density of all PZT films

图 6. 所有 PZT 薄膜的漏电流密度

4. 结论

使用磁控溅射法成功的在 $\text{Pb}_{1.10}(\text{Zr}_{0.52}, \text{Ti}_{0.48})\text{O}_3$ 作为种子层，Pt(111)/Ti/SiO₂/Si(100) 基底上制备了由 $0.3\text{Pb}(\text{Mg}_{1/3}\text{Nb}_{2/3})\text{O}_3$ - $0.7\text{Pb}(\text{Zr}_{0.52}\text{Ti}_{0.48})\text{O}_3$ 和 $\text{Pb}(\text{Zr}_{0.52}\text{Ti}_{0.48})\text{O}_3$ 组成的铁电多层薄膜。经 XRD 分析，多层薄膜的(111)择优取向度较高。SEM 图显示薄膜有着致密均匀的柱状结构的钙钛矿相。PMN-PZT 与 PZT 的

厚度比为 2:1 的多层异质薄膜具有最佳的介电性能, $\epsilon_r = 1237.9$ 和 $\tan\delta = 0.046$ 。PMN-PZT 和 PZT 的厚度比为 2:1 的多层异质薄膜相比其它薄膜具有更好的铁电性能, $P_r = 21.3 \mu\text{C}/\text{cm}^2$, $E_c = 88.1\text{KV}/\text{cm}$ 。此外, PMN-PZT 和 PZT 的厚度比为 2:1 的多层异质薄膜在电场作用下的漏电流密度最小, $J = 5.5 \times 10^{-8} \text{A}/\text{cm}^2$ 。

参考文献

- [1] Haertling, G.H. (1999) Ferroelectric Ceramics: History and Technology. *Journal of the American Ceramic Society*, **82**, 797-818. <https://doi.org/10.1111/j.1151-2916.1999.tb01840.x>
- [2] 孙慷, 张幅学. 压电学[M]. 北京: 国防工业出版社, 1984: 117-120.
- [3] Izyumskaya, N., Alivov, Y., Cho, S.J., Morkoç, H., Lee, H. and Kang, Y.-S. (2007) Processing, Structure, Properties, and Applications of PZT Thin Films. *Critical Reviews in Solid State and Materials Sciences*, **32**, 111-202. <https://doi.org/10.1080/10408430701707347>
- [4] He, B. and Wang, Z. (2016) Enhancement of the Electrical Properties in $\text{BaTiO}_3/\text{PbZr}_{0.52}\text{Ti}_{0.48}\text{O}_3$ Ferroelectric Superlattices. *ACS Applied Materials & Interfaces*, **8**, 6736-6742. <https://doi.org/10.1021/acsami.5b12098>
- [5] Datta, A., Mukherjee, D., Witanachchi, S. and Mukherjee, P. (2014) Hierarchically Ordered Nano-Hetero Structured PZT Thin Films with Enhanced Ferroelectric Properties. *Advanced Functional Materials*, **24**, 2638-2647. <https://doi.org/10.1002/adfm.201303290>
- [6] Vrejoiu, I., Zhu, Y., Rhun, G.L., Andreas Schubert, M., Hesse, D. and Alexe, M. (2007) Structure and Properties of Epitaxial Ferroelectric $\text{PbZr}_{0.4}\text{Ti}_{0.6}\text{O}_3/\text{PbZr}_{0.6}\text{Ti}_{0.4}\text{O}_3$ Superlattices Grown on SrTiO_3 (001) by Pulsed Laser Deposition. *Applied Physics Letters*, **90**, Article ID: 072909. <https://doi.org/10.1063/1.2643259>
- [7] 赵海波. 水热合成法制备 PZT 压电薄膜的研究[D]: [硕士学位论文]. 大连: 大连理工大学, 2006.
- [8] Ma, B., Liu, S., Tong, S., Narayanan, M. and (Balu) Balachandran, U. (2012) Enhanced Dielectric Properties of $\text{Pb}_{0.92}\text{La}_{0.08}\text{Zr}_{0.52}\text{Ti}_{0.48}\text{O}_3$ Films with Compressive Stress. *Journal of Applied Physics*, **112**, Article ID: 114117. <https://doi.org/10.1063/1.4768926>
- [9] Masruroh (2013) Influence of the Waveform and DC Offset on the Asymmetric Hysteresis Loop in $\text{Au}/\text{PZT}/\text{Pt}/\text{Al}_2\text{O}_3/\text{SiO}_2/\text{Si}$ Thin Films Prepared by MOCVD Method. *Applied Mechanics and Materials*, **467**, 155-159. <https://doi.org/10.4028/www.scientific.net/AMM.467.155>
- [10] Kingon, A.I. and Srinivasan, S. (2005) Lead Zirconate Titanate Thin Films Directly on Copper Electrodes for Ferroelectric, Dielectric and Piezoelectric Applications. *Nature Materials*, **4**, 233-237. <https://doi.org/10.1038/nmat1334>
- [11] Kim, J., Yang, S.A., Choi, Y.C., Han, J.K., Jeong, K.O., Yun, Y.J., et al. (2008) Ferroelectricity in Highly Ordered Arrays of Ultra-Thin-Walled $\text{Pb}(\text{Zr},\text{Ti})\text{O}_3$ Nanotubes Composed of Nanometer-Sized Perovskite Crystallites. *Nano Letters*, **8**, 1813-1818. <https://doi.org/10.1021/nl080240t>
- [12] Higuchi, K., Miyazawa, K., Sakuma, T. and Suzuki, K. (1994) Microstructure Characterization of Sol-Gel Derived PZT Films. *Journal of Materials Science*, **29**, 436-441. <https://doi.org/10.1007/BF01162503>
- [13] Fujii, T., Hishinuma, Y., Mita, T. and Naono, T. (2010) Characterization of Nb-Doped $\text{Pb}(\text{Zr},\text{Ti})\text{O}_3$ Films Deposited on Stainless Steel and Silicon Substrates by RF-Magnetron Sputtering for MEMS Applications. *Sensors and Actuators A: Physical*, **163**, 220-225. <https://doi.org/10.1016/j.sna.2010.08.019>
- [14] Krupanidhi, S.B., Maffei, N., Sayer, M. and El-Assal, K. (2011) R.F. Magnetron Sputtering of Ferroelectric PZT Films. *Ferroelectrics*, **51**, 93-98. <https://doi.org/10.1080/00150198308009058>
- [15] Han, H., Song, X., Zhong, J., Kotru, S., Padmini, P. and Pandey, R.K. (2004) Highly α -Axis-Oriented Nb-Doped $\text{Pb}(\text{Ti}_x\text{Zr}_{1-x})\text{O}_3$ Thin Films Grown by Sol-gel Technique for Uncooled Infrared Detectors. *Applied Physics Letters*, **85**, 5310-5312. <https://doi.org/10.1063/1.1825062>
- [16] Wang, Z.J., Kokawa, H. and Maeda, R. (2005) *In Situ* Growth of Lead Zirconate Titanate Thin Films by Hybrid Process: Sol-gel Method and Pulsed-Laser Deposition. *Acta Materialia*, **53**, 593-600. <https://doi.org/10.1016/j.actamat.2004.10.012>
- [17] Wang, Z.J., Kokawa, H., Takizawa, H., Ichiki, M. and Maeda, R. (2005) Low-Temperature Growth of High-Quality Lead Zirconate Titanate Thin Films by 28 GHz Microwave Irradiation. *Applied Physics Letters*, **86**, Article ID: 212903. <https://doi.org/10.1063/1.1935748>
- [18] Kanda, K., Hirai, S., Fujita, T. and Maenaka, K. (2018) Piezoelectric MEMS with Multilayered $\text{Pb}(\text{Zr},\text{Ti})\text{O}_3$ Thin Films for Energy Harvesting. *Sensors and Actuators A: Physical*, **281**, 229-235. <https://doi.org/10.1016/j.sna.2018.09.018>
- [19] Bousquet, E., Dawber, M., Stucki, N., Lichtensteiger, C., Hermet, P., Gariglio, S., et al. (2008) Improper Ferroelectricity in Perovskite Oxide Artificial Superlattices. *Nature*, **452**, 732-736. <https://doi.org/10.1038/nature06817>

- [20] Xu, H., Feng, M., Liu, M., Sun, X., Wang, L., Jiang, L., *et al.* (2018) Strain-Mediated Converse Magnetoelectric Coupling in $\text{La}_{0.7}\text{Sr}_{0.3}\text{MnO}_3/\text{Pb}(\text{Mg}_{1/3}\text{Nb}_{2/3})\text{O}_3\text{-PbTiO}_3$ Multiferroic Heterostructures. *Crystal Growth & Design*, **18**, 5934-5939. <https://doi.org/10.1021/acs.cgd.8b00702>
- [21] Tang, Y., Zhu, B., Wang, F., Sun, D., Hu, Z., Qin, X., *et al.* (2016) Dielectric and Ferroelectric Properties of (111) Preferred Oriented $\text{PbZr}_{0.53}\text{Ti}_{0.47}\text{O}_3/\text{Pb}(\text{Mg}_{1/3}\text{Nb}_{2/3})_{0.62}\text{Ti}_{0.38}\text{O}_3/\text{PbZr}_{0.53}\text{Ti}_{0.47}\text{O}_3$ Trilayered Films. *Applied Surface Science*, **371**, 160-163. <https://doi.org/10.1016/j.apsusc.2016.02.213>
- [22] Zhang, T., Zhang S-Y, Wasa, K., Zhang, H., Chen, Z.-J., Shui, X.-J. *et al.* (2011) Effects of $\text{Pb}(\text{Mn,Nb})\text{O}_3$ Doping on the Properties of PZT-Based Films Deposited on Silicon Substrates. *Physica Status Solidi (A)*, **208**, 2460-2466. <https://doi.org/10.1002/pssa.201026561>
- [23] Lian, J., Ponchel, F., Tiercelin, N., Han, L., Chen, Y., Rémiens, D., *et al.* (2018) Influence of the Magnetic State on the Voltage-Controlled Magnetoelectric Effect in A Multiferroic Artificial Heterostructure YIG/PMN-PZT. *Journal of Applied Physics*, **124**, Article ID: 064101. <https://doi.org/10.1063/1.5037057>
- [24] 许立宁. 基于 MEMS 技术的压电微喷的研制[D]: [博士学位论文]. 北京: 中国科学院研究生院(电子学研究所), 2005.
- [25] Yang, F., Fei, W.D. and Sun, Q. (2009) Highly (100)-Textured $\text{Pb}(\text{Zr}_{0.52}\text{Ti}_{0.48})\text{O}_3$ Film Derived From A Modified Sol-gel Technique Using Inorganic Zirconium Precursor. *Journal of Materials Processing Technology*, **209**, 220-224. <https://doi.org/10.1016/j.jmatprotec.2008.01.042>
- [26] Es-Souni, M., Abed, M., Solterbeck, C.H. and Piorra, A (2002) Crystallization Kinetics and Dielectric Properties of Solution Deposited, La Doped PZT Thin Films. *Materials Science and Engineering B-Solid State Materials for Advanced Technology*, **94**, 229-236. [https://doi.org/10.1016/S0921-5107\(02\)00099-5](https://doi.org/10.1016/S0921-5107(02)00099-5)
- [27] Kanno, I. (2018) Piezoelectric MEMS: Ferroelectric Thin Films for MEMS Applications. *Japanese Journal of Applied Physics*, **57**, Article ID: 040101. <https://doi.org/10.7567/JJAP.57.040101>